

# The energy spectrum of cosmic-ray electrons at TeV energies

F. Aharonian<sup>1,13</sup>, A.G. Akhperjanian<sup>2</sup>, U. Barres de Almeida<sup>8,\*</sup>, A.R. Bazer-Bachi<sup>3</sup>, Y. Becherini<sup>12</sup>, B. Behera<sup>14</sup>, W. Benbow<sup>1</sup>, K. Bernlöhr<sup>1,5</sup>, C. Boisson<sup>6</sup>, A. Bochow<sup>1</sup>, V. Borrel<sup>3</sup>, I. Braun<sup>1</sup>, E. Brion<sup>7</sup>, J. Brucker<sup>16</sup>, P. Brun<sup>7</sup>, R. Bühler<sup>1</sup>, T. Bulik<sup>24</sup>, I. Büsching<sup>9</sup>, T. Boutelier<sup>17</sup>, S. Carrigan<sup>1</sup>, P.M. Chadwick<sup>8</sup>, A. Charbonnier<sup>19</sup>, R.C.G. Chaves<sup>1</sup>, A. Cheesebrough<sup>8</sup>, L.-M. Chounet<sup>10</sup>, A.C. Clapson<sup>1</sup>, G. Coignet<sup>11</sup>, L. Costamante<sup>1,29</sup>, M. Dalton<sup>5</sup>, B. Degrange<sup>10</sup>, C. Deil<sup>1</sup>, H.J. Dickinson<sup>8</sup>, A. Djannati-Atai<sup>12</sup>, W. Domainko<sup>1</sup>, L.O'C. Drury<sup>13</sup>, F. Dubois<sup>11</sup>, G. Dubus<sup>17</sup>, J. Dyks<sup>24</sup>, M. Dyrda<sup>28</sup>, K. Egberts<sup>1,†</sup>, D. Emmanoulopoulos<sup>14</sup>, P. Espigat<sup>12</sup>, C. Farnier<sup>15</sup>, F. Feinstein<sup>15</sup>, A. Fiasson<sup>15</sup>, A. Förster<sup>1</sup>, G. Fontaine<sup>10</sup>, M. Füßling<sup>5</sup>, S. Gabici<sup>13</sup>, Y.A. Gallant<sup>15</sup>, L. Gérard<sup>12</sup>, B. Giebels<sup>10</sup>, J.F. Glicenstein<sup>7</sup>, B. Glück<sup>16</sup>, P. Goret<sup>7</sup>, C. Hadjichristidis<sup>8</sup>, D. Hauser<sup>14</sup>, M. Hauser<sup>14</sup>, S. Heinz<sup>16</sup>, G. Heinzlmann<sup>4</sup>, G. Henri<sup>17</sup>, G. Hermann<sup>1</sup>, J.A. Hinton<sup>25</sup>,<sup>‡</sup> A. Hoffmann<sup>18</sup>, W. Hofmann<sup>1</sup>, M. Holleran<sup>9</sup>, S. Hoppe<sup>1</sup>, D. Horns<sup>4</sup>, A. Jacholkowska<sup>19</sup>, O.C. de Jager<sup>9</sup>, I. Jung<sup>16</sup>, K. Katarzyński<sup>27</sup>, S. Kaufmann<sup>14</sup>, E. Kendziorra<sup>18</sup>, M. Kerschhaggl<sup>15</sup>, D. Khangulyan<sup>1</sup>, B. Khélifi<sup>10</sup>, D. Keogh<sup>8</sup>, Nu. Komin<sup>15</sup>, K. Kosack<sup>1</sup>, G. Lamanna<sup>11</sup>, J.-P. Lenain<sup>6</sup>, T. Lohse<sup>5</sup>, V. Marandon<sup>12</sup>, J.M. Martin<sup>6</sup>, O. Martineau-Huynh<sup>19</sup>, A. Marcowith<sup>15</sup>, D. Maurin<sup>19</sup>, T.J.L. McComb<sup>8</sup>, C. Medina<sup>6</sup>, R. Moderski<sup>24</sup>, E. Moulin<sup>7</sup>, M. Naumann-Godo<sup>10</sup>, M. de Naurois<sup>19</sup>, D. Nedbal<sup>20</sup>, D. Nekrassov<sup>1</sup>, J. Niemiec<sup>28</sup>, S.J. Nolan<sup>8</sup>, S. Ohm<sup>1</sup>, J.-F. Olive<sup>3</sup>, E. de Oña Wilhelmi<sup>12</sup>, K.J. Orford<sup>8</sup>, J.L. Osborne<sup>8</sup>, M. Ostrowski<sup>23</sup>, M. Panter<sup>1</sup>, G. Pedalletti<sup>14</sup>, G. Pelletier<sup>17</sup>, P.-O. Petrucci<sup>17</sup>, S. Pita<sup>12</sup>, G. Pühlhofer<sup>14</sup>, M. Punch<sup>12</sup>, A. Quirrenbach<sup>14</sup>, B.C. Raubenheimer<sup>9</sup>, M. Raue<sup>1,29</sup>, S.M. Rayner<sup>8</sup>, M. Renaud<sup>1</sup>, F. Rieger<sup>1,29</sup>, J. Ripken<sup>4</sup>, L. Rob<sup>20</sup>, S. Rosier-Lees<sup>11</sup>, G. Rowell<sup>26</sup>, B. Rudak<sup>24</sup>, C.B. Rulten<sup>8</sup>, J. Ruppel<sup>21</sup>, V. Sahakian<sup>2</sup>, A. Santangelo<sup>18</sup>, R. Schlickeiser<sup>21</sup>, F.M. Schöck<sup>16</sup>, R. Schröder<sup>21</sup>, U. Schwanke<sup>5</sup>, S. Schwarzburg<sup>18</sup>, S. Schwemmer<sup>14</sup>, A. Shalchi<sup>21</sup>, J.L. Skilton<sup>25</sup>, H. Sol<sup>6</sup>, D. Spangler<sup>8</sup>, L. Stawarz<sup>23</sup>, R. Steenkamp<sup>22</sup>, C. Stegmann<sup>16</sup>, G. Superina<sup>10</sup>, P.H. Tam<sup>14</sup>, J.-P. Tavernier<sup>19</sup>, R. Terrier<sup>12</sup>, O. Tibolla<sup>14</sup>, C. van Eldik<sup>1</sup>, G. Vasileiadis<sup>15</sup>, C. Venter<sup>9</sup>, J.P. Vialle<sup>11</sup>, P. Vincent<sup>19</sup>, M. Vivier<sup>7</sup>, H.J. Völk<sup>1</sup>, F. Volpe<sup>10,29</sup>, S.J. Wagner<sup>14</sup>, M. Ward<sup>8</sup>, A.A. Zdziarski<sup>24</sup>, and A. Zech<sup>6</sup>

<sup>1</sup> *Max-Planck-Institut für Kernphysik, P.O. Box 103980, D 69029 Heidelberg, Germany*

<sup>2</sup> *Yerevan Physics Institute, 2 Alikhanian Brothers St., 375036 Yerevan, Armenia*

<sup>3</sup> *Centre d'Etude Spatiale des Rayonnements, CNRS/UPS,*

*9 av. du Colonel Roche, BP 4346, F-31029 Toulouse Cedex 4, France*

<sup>4</sup> *Universität Hamburg, Institut für Experimentalphysik,*

*Luruper Chaussee 149, D 22761 Hamburg, Germany*

<sup>5</sup> *Institut für Physik, Humboldt-Universität zu Berlin, Newtonstr. 15, D 12489 Berlin, Germany*

<sup>6</sup> *LUTH, Observatoire de Paris, CNRS, Université Paris Diderot, 5 Place Jules Janssen, 92190 Meudon, France*

<sup>7</sup> *IRFU/DSM/CEA, CE Saclay, F-91191 Gif-sur-Yvette, Cedex, France*

<sup>8</sup> *University of Durham, Department of Physics, South Road, Durham DH1 3LE, U.K.*

<sup>9</sup> *Unit for Space Physics, North-West University, Potchefstroom 2520, South Africa*

<sup>10</sup> *Laboratoire Leprince-Ringuet, Ecole Polytechnique, CNRS/IN2P3, F-91128 Palaiseau, France*

<sup>11</sup> *Laboratoire d'Annecy-le-Vieux de Physique des Particules, CNRS/IN2P3,*

*9 Chemin de Bellevue - BP 110 F-74941 Annecy-le-Vieux Cedex, France*

<sup>12</sup> *Astroparticule et Cosmologie (APC), CNRS, Université Paris 7 Denis Diderot,*

*10, rue Alice Domon et Leonie Duquet, F-75205 Paris Cedex 13, France* <sup>§</sup>

<sup>13</sup> *Dublin Institute for Advanced Studies, 5 Merrion Square, Dublin 2, Ireland*

<sup>14</sup> *Landessternwarte, Universität Heidelberg, Königstuhl, D 69117 Heidelberg, Germany*

<sup>15</sup> *Laboratoire de Physique Théorique et Astroparticules,*

*CNRS/IN2P3, Université Montpellier II, CC 70,*

*Place Eugène Bataillon, F-34095 Montpellier Cedex 5, France*

<sup>16</sup> *Universität Erlangen-Nürnberg, Physikalisches Institut,*

*Erwin-Rommel-Str. 1, D 91058 Erlangen, Germany*

<sup>17</sup> *Laboratoire d'Astrophysique de Grenoble, INSU/CNRS,*

*Université Joseph Fourier, BP 53, F-38041 Grenoble Cedex 9, France*

<sup>18</sup> *Institut für Astronomie und Astrophysik, Universität Tübingen, Sand 1, D 72076 Tübingen, Germany*

<sup>19</sup> *LPNHE, Université Pierre et Marie Curie Paris 6,*

*Université Denis Diderot Paris 7, CNRS/IN2P3,*

*4 Place Jussieu, F-75252, Paris Cedex 5, France*

<sup>20</sup> *Institute of Particle and Nuclear Physics, Charles University,*

*V Holesovickach 2, 180 00 Prague 8, Czech Republic*

<sup>21</sup> *Institut für Theoretische Physik, Lehrstuhl IV: Weltraum und Astrophysik,*

*Ruhr-Universität Bochum, D 44780 Bochum, Germany*

<sup>22</sup> *University of Namibia, Private Bag 13301, Windhoek, Namibia*

<sup>23</sup> *Observatorium Astronomiczne, Uniwersytet Jagielloński, Kraków, Poland*

<sup>24</sup> *Nicolaus Copernicus Astronomical Center, Warsaw, Poland*

<sup>25</sup> *School of Physics & Astronomy, University of Leeds, Leeds LS2 9JT, UK*

<sup>26</sup> *School of Chemistry & Physics, University of Adelaide, Adelaide 5005, Australia*

<sup>27</sup> *Toruń Centre for Astronomy, Nicolaus Copernicus University, Toruń, Poland*

<sup>28</sup> *Instytut Fizyki Jądrowej PAN, ul. Radzikowskiego 152, 31-342 Kraków, Poland and*

<sup>29</sup> *European Associated Laboratory for Gamma-Ray Astronomy, jointly supported by CNRS and MPG*

The very large collection area of ground-based  $\gamma$ -ray telescopes gives them a substantial advantage over balloon/satellite based instruments in the detection of very-high-energy ( $>600$  GeV) cosmic-ray electrons. Here we present the electron spectrum derived from data taken with the H.E.S.S. system of imaging atmospheric Cherenkov telescopes. In this measurement, the first of this type, we are able to extend the measurement of the electron spectrum beyond the range accessible to direct measurements. We find evidence for a substantial steepening in the energy spectrum above 600 GeV compared to lower energies.

PACS numbers: 95.85.Ry

In stark contrast to hadronic cosmic rays (CRs) the lifetime and hence propagation distance of CR electrons in the very-high-energy regime is severely limited by energy losses via synchrotron radiation and inverse Compton scattering. The lifetime of a very-high-energy electron can be expressed as:  $t \approx 5 \times 10^5 (E/1 \text{ TeV})^{-1} ((B/5 \mu\text{G})^2 + 1.6 (w/1 \text{ eV cm}^{-3}))^{-1}$  years, where  $w$  is the energy density in low frequency photons ( $h\nu \ll 0.1 \text{ eV}$ ) in the interstellar medium and  $B$  is the mean interstellar magnetic field. In standard diffusion-dominated models of Galactic cosmic-ray transport this implies that the sources of TeV electrons must be local ( $< 1 \text{ kpc}$  distance) as discussed in e.g. [1] and [2]. A second consequence of these energy-dependent losses is that the electron spectrum is *steeper* than that of the hadronic CRs ( $\sim E^{-3.3}$  cf.  $E^{-2.7}$ ). All measurements so far have utilized balloon or satellite borne instrumentation (see [3] for a review). However, the rapidly declining flux makes such direct measurements at high energies difficult. It has been suggested ([4]) that the very large collection area of ground-based imaging atmospheric Cherenkov telescope (IACT) arrays could be used to extend CR electron spectrum measurements into the TeV domain. The challenge for such instruments (as indeed for all CR electron measurements) is to recognize electrons against the much more numerous background of hadronic CRs. The recent improvements in hadron-rejection power achieved by the High Energy Stereoscopic System (H.E.S.S.) instrument have now made such a measurement possible.

H.E.S.S. is an array of four imaging atmospheric Cherenkov telescopes situated in the Khomas Highland of Namibia [5]. The array is sensitive to  $\gamma$ -rays (and electrons) above a threshold of  $\approx 100 \text{ GeV}$ . The sensitivity of the array to extended  $\gamma$ -ray emission has been demonstrated with the mapping of supernova remnant shells ([6], [7]), and the diffuse emission around the Galactic Center [8]. The factor  $\sim 10$  improvement in  $\gamma$ -ray flux sensitivity of H.E.S.S. over previous generation experiments is based largely on superior rejection of the hadronic background. Because this measurement does not discriminate between electrons and positrons, *electrons* is used generically in the following to refer to both particle and anti-particle. The H.E.S.S. electron analysis presented here is based on the selection of *electron-*

*like* events in regions far from  $\gamma$ -ray sources and subtraction of the remaining hadronic CR background using air-shower simulations. The data used were acquired using the complete 4-telescope array during 2004 to 2007. All data passing quality selection criteria, with zenith angles smaller than  $28^\circ$ , and targeting extragalactic sources, were used in this analysis, amounting to 239 hours of live-time. Only the central  $3.0^\circ$  of the field-of-view was utilized, with regions within  $0.4^\circ$  of any known or potential  $\gamma$ -ray source excluded. The energy is reconstructed using standard methods. The effective collection area using the technique described below is energy dependent and reaches  $\approx 5 \times 10^4 \text{ m}^2$  at 1 TeV. The total effective exposure of this data set at 1 TeV is therefore  $\approx 8.5 \times 10^7 \text{ m}^2 \text{ sr s}$ .

The most critical aspect of electron analysis is the efficient rejection of the hadronic background. Given the relatively high flux of cosmic electrons with respect to typical  $\gamma$ -ray sources it is appropriate to make tight selection cuts to achieve the best possible signal/background ratio. Very hard event selection, including the requirement that all four H.E.S.S. telescopes triggered in the event, leads to a greatly increased energy threshold of  $\approx 600 \text{ GeV}$ . A *Random Forest* [9] (see also [10]) approach was used to convert image information from the four cameras into a single parameter  $\zeta$  describing the degree to which a shower is *electron-like*. The primary input parameters to the Random Forest algorithm are the Hillas moments [11] of the images recorded in each telescope. A  $\zeta$  value of zero corresponds to a shower which is almost certainly background, and a value of one is assigned if the shower is almost certainly an electron. Random Forests were trained in five energy bands using simulated electron showers and data taken from empty regions. To subtract the hadronic background the  $\zeta$  distribution of protons and nuclei must be known. For this purpose sets of  $10^{10}$  proton showers and showers of heavier nuclei were simulated with CORSIKA [12] using both the SIBYLL [13] and QGSJET-II [14] interaction models. About  $10^{-2}$  of these showers trigger the array, and due to the extremely efficient background rejection, only  $10^{-6}$  fall into the regime  $\zeta > 0.9$ . While a component of heavier nuclei is required to explain the distribution of  $\zeta$  at values up to 0.5, the background can be considered as purely protonic at larger values of  $\zeta$ .

Fig. 1 shows the measured distribution of the param-

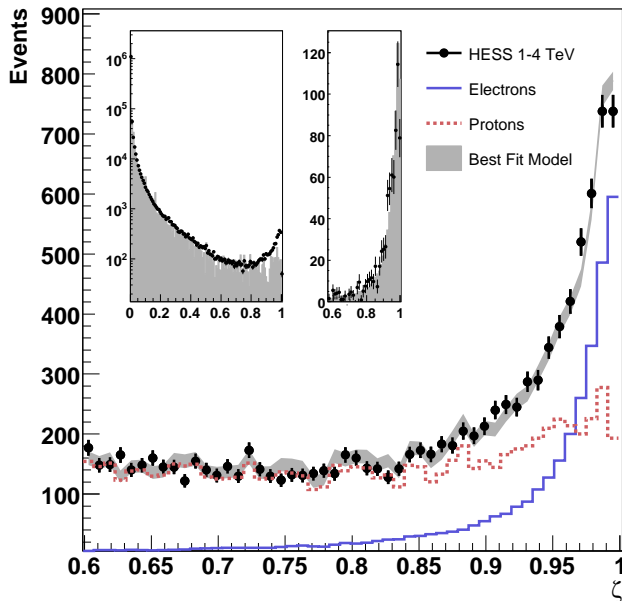


FIG. 1: The measured distribution of the parameter  $\zeta$ , compared with distributions for simulated protons and electrons, for showers with reconstructed energy between 1 and 4 TeV. The best fit model combination of electrons and protons is shown as a shaded band. The proton simulations use the SIBYLL hadronic interaction event generator. The left inset shows the complete distribution from zero to one with entries on a log scale; the data are shown as points, the filled histogram shows a mixed composition (proton, He, N, Si & Fe) cosmic-ray model. To demonstrate the match between simulation and data in electromagnetic showers, the right inset shows background subtracted  $\gamma$ -ray data as points and  $\gamma$ -ray simulations as filled histogram.

eter  $\zeta$  compared with the simulated distributions for the energy range 1–4 TeV. The peak close to  $\zeta = 1$  is evidence of a diffuse component of purely-electromagnetic showers at these energies. The data at  $\zeta > 0.6$  can be described by a combination of simulated electrons and protons. By fitting the  $\zeta$  distribution of the data with the distributions of simulated electrons and protons in independent energy bands (with two free parameters being the electron and proton contribution), the most probable number of measured electron showers in each energy band can be deduced. The total normalized goodness-of-fit in the  $\zeta$  range of 0.6–1 for reconstructed energies between 1 and 4 TeV is  $\chi^2/\nu = 0.98$  for a model of simulated electrons and protons using SIBYLL (probability  $p = 0.5$ ) and 2.15 for a model using QGSJET-II ( $p = 1.7 \times 10^{-4}$ ), which demonstrates that the SIBYLL model provides a better description of measurable parameters of air showers initiated by protons of TeV energies. Coupled with the knowledge of the energy-dependent effective collection area, which is obtained from electron simulations following a powerlaw with a spectral index of 3.3, the number of measured electron showers can be used to determine the primary electron spectrum. As electron-

initiated air showers are in practice extremely difficult to separate from  $\gamma$ -ray showers, the peak in our data at  $\zeta = 1$  may contain a contribution from  $\gamma$ -ray showers. The signal measured by H.E.S.S. (close to  $\zeta = 1$ ) is therefore a combination of the CR electron flux (CREF) and the extragalactic  $\gamma$ -ray background (EGRB). The level of the EGRB lies many orders of magnitude below the CREF at GeV energies but a naive extrapolation of the last few data points measured by EGRET [15] yields an  $dN/dE \propto E^{-2}$  spectrum which reaches the level of the CREF at a few TeV. However, most models for the EGRB yield TeV fluxes at least one order of magnitude lower than this extrapolation (see for example [16]). The predicted flux of inverse Compton scattered solar photons off CR electrons is also negligible due to our geometry pointing away from the Sun [17]. Given the uncertainty in the EGRB/CREF ratio at TeV energies it is desirable to separate electrons and  $\gamma$ -rays in our data. Essentially the only useful separation parameter is the depth of shower maximum ( $X_{\max}$ ), which occurs on average  $\approx 20 \text{ g cm}^{-2}$  (or  $\sim$  half a radiation length) higher in the atmosphere for electrons. Fig. 2 compares reconstructed  $X_{\max}$  distributions for simulated protons, electrons and  $\gamma$ -rays to the experimentally measured  $X_{\max}$  distribution for electron-like events ( $\zeta > 0.9$ ). A fit of the  $X_{\max}$  distribution with the electron/ $\gamma$ -ray fraction as a free parameter results in a maximum 10% contribution of  $\gamma$ -rays to the signal (for a confidence level of 90%), which is supported by the displacement between the  $X_{\max}$  distributions from data used for this electron analysis and data from a  $\gamma$ -ray rich data set (inset of Fig. 2). However, taking into account a conservative systematic uncertainty in the determination of  $X_{\max}$  of  $5 \text{ g cm}^{-2}$  due to atmospheric uncertainties, we cannot exclude a significant contamination of  $\approx 50\%$  of our electron measurement by the diffuse extragalactic  $\gamma$ -ray background. Systematic uncertainties in the hadronic modeling are not considered.

Fig. 3 shows the CR electron spectrum derived from this analysis together with a compilation of earlier measurements. Systematic errors on the reconstructed spectrum arise from uncertainties in the simulation of hadronic interactions and the atmospheric model, as well as in the absolute energy scale. The energy scale uncertainty is  $\approx 15\%$  and is illustrated by a double arrow in Fig. 3. The uncertainty arising from the subtraction of the hadronic background has been estimated by comparison of the spectra obtained using the SIBYLL and QGSJET-II models. The  $\zeta$  distributions for protons show a slight rise toward  $\zeta = 1$  (see Fig. 1), presumably reflecting events where a large fraction of proton energy is transformed to a single  $\pi^0$ . The rise is somewhat more pronounced for SIBYLL as compared to QGSJET-II, giving rise to the model dependence. Artificially doubling the  $\gamma$ -ray like component in SIBYLL reduces the electron flux by  $\sim 20\%$ , without significant

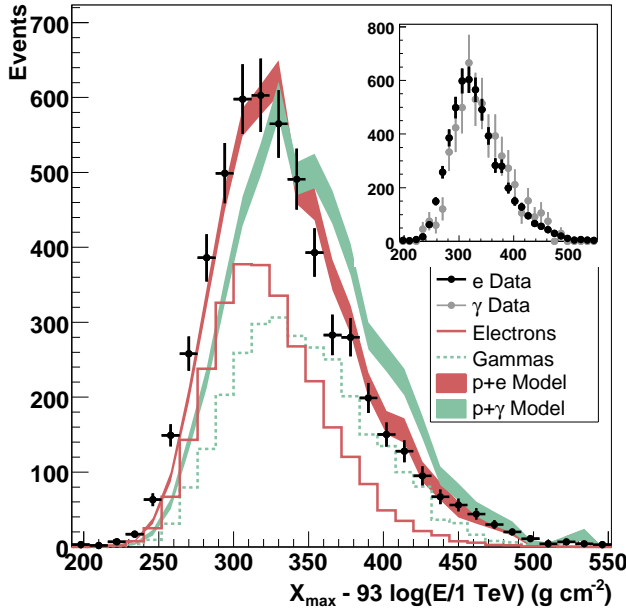


FIG. 2: The distribution of reconstructed shower maximum ( $X_{\max}$ ) for H.E.S.S. data, compared to simulations. For each shower the measured  $X_{\max}$  is corrected for the energy dependent shower elongation ( $93 \text{ g cm}^{-2}/\text{decade}$  is the reconstructed elongation rate expected for electron primaries). Showers with reconstructed energies between 1 and 4 TeV are included. The bands show the combination of electrons and protons (simulated using SIBYLL) and of  $\gamma$ -rays and protons, with a ratio determined by a fit to the  $\zeta$  distribution of the data in this energy range. The distributions of electrons and  $\gamma$ -rays are shown for comparison. The inset contains a comparison of this data (black) with a  $\gamma$ -ray rich data set taken from regions  $< 0.15^\circ$  from  $\gamma$ -ray sources (gray).

change in spectral shape. Detailed tests of the analysis using different zenith angle ranges, different analysis cuts (variations of the cuts on  $\zeta$ , the maximum impact distance of the showers and the minimal intensity of the shower image in the camera), different regions in the sky, different seasons and years as well as another fitting algorithm all yield consistent results. The estimated systematic errors, apart from the 15% scale uncertainty, are illustrated by the shaded band in Fig. 3. Our data are well described by a power-law:  $dN/dE = k(E/1\text{TeV})^{-\Gamma}$  with  $k = (1.17 \pm 0.02) \times 10^{-4} \text{ TeV}^{-1} \text{ m}^{-2} \text{ sr}^{-1} \text{ s}^{-1}$  and  $\Gamma = 3.9 \pm 0.1$  (stat) ( $\chi^2/\nu = 3.6$ ,  $p = 10^{-3}$ , Fit A), which implies a steepening of the spectrum compared to GeV energies. The spectral index shows little model and sample dependence, resulting in  $\Delta\Gamma(\text{syst.}) \lesssim 0.3$ . At lower energies the flux reported here is somewhat higher than previous results, but fully consistent within the 15% scale error. Leaving the scale factor free, H.E.S.S. data combined with earlier electron data are well reproduced by an exponentially cutoff powerlaw with an index of  $-3.05 \pm 0.02$  and a cutoff at  $2.1 \pm 0.3 \text{ TeV}$ , combined with a scale adjustment of  $-11\%$  (Fit B). H.E.S.S. data are also compatible with very recent ATIC data [22], but

due to the limited energy range no conclusion can be drawn concerning the existence of a step in the spectrum as claimed by ATIC.

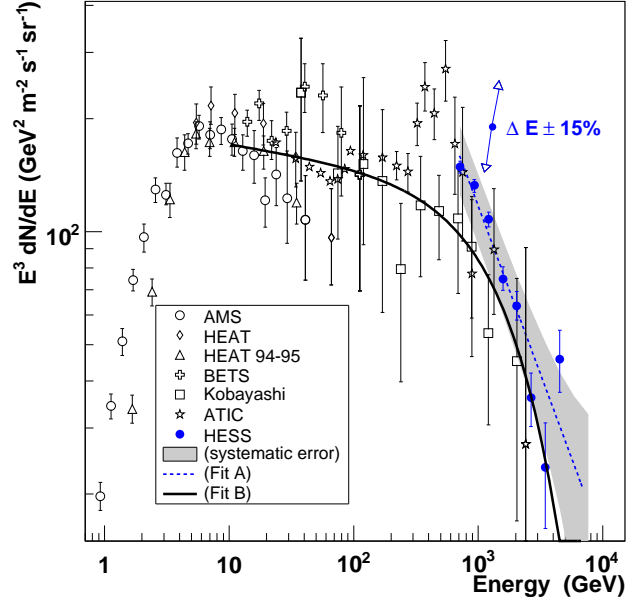


FIG. 3: The energy spectrum  $E^3 dN/dE$  of CR electrons as measured by H.E.S.S. in comparison with previous measurements. The H.E.S.S. data are shown as solid points. The two fit functions (A and B) are described in the main text. Upper limits are given for a confidence level of 95%. The shaded band indicates the approximate systematic error arising from uncertainties in the modeling of hadronic interactions and in the atmospheric model. The double arrow indicates the effect of an energy scale shift of 15%, the approximate systematic uncertainty on the H.E.S.S. points. Previous data are reproduced from: AMS [18], HEAT [19], HEAT 94-95 [20], BETS [21], Kobayashi [2] and ATIC [22].

Whilst the detailed interpretation of this result is beyond the scope of this paper, we note that our measurement implies the existence of at least one source of CR electrons in the local Galaxy (within  $\sim 1 \text{ kpc}$ ). Some scenarios of a strong local source [2] are excluded. This measurement is the first ground-based measurement of CR electrons. Future IACT arrays with effective areas beyond  $10^6 \text{ m}^2$  should be able to extend the spectrum to 10 TeV using this technique.

The support of the Namibian authorities and of the University of Namibia in facilitating the construction and operation of H.E.S.S. is gratefully acknowledged, as is the support by the German Ministry for Education and Research (BMBF), the Max Planck Society, the French Ministry for Research, the CNRS-IN2P3 and the Astroparticle Interdisciplinary Programme of the CNRS, the U.K. Science and Technology Facilities Council (STFC), the IPNP of the Charles University, the Polish Ministry of Science and Higher Education, the South African Department of Science and Technology and National Research Foundation, and by the University of Namibia.

We appreciate the excellent work of the technical support staff in Berlin, Durham, Hamburg, Heidelberg, Palaiseau, Paris, Saclay, and in Namibia in the construction and operation of the equipment.

---

\* supported by CAPES Foundation, Ministry of Education of Brazil

<sup>†</sup> Electronic address: Kathrin.Egberts@mpi-hd.mpg.de

<sup>‡</sup> Electronic address: j.a.hinton@leeds.ac.uk

<sup>§</sup> UMR 7164 (CNRS, Université Paris VII, CEA, Observatoire de Paris)

- [1] F. A. Aharonian, A. M. Atoyan, H. J. Völk, *Astron. & Astrophys.*, **294**, L41 (1995).
- [2] T. Kobayashi *et al.*, *Astrophys. J.*, **601**, 340 (2004).
- [3] D. Müller, *Adv. Space Res.*, **27**, 659 (2001).
- [4] J. Nishimura, *Proc. Towards a Major Cherenkov Detector III*, Universal Academy Press, Tokyo, page 1 (1994).
- [5] J. A. Hinton (*H.E.S.S. Collaboration*), *New Astron. Rev.* **48**, 331 (2004).
- [6] F. A. Aharonian *et al.*, *Nature* **432**, 75 (2004).
- [7] F. A. Aharonian *et al.*, *Astron. & Astrophys.* **437**, L7 (2005).
- [8] F. A. Aharonian *et al.*, *Nature* **439**, 695 (2006).
- [9] L. Breiman & A. Cutler, <http://www.stat.berkeley.edu/users/breiman/RandomForests/>
- [10] R. K. Bock *et al.*, *NIM A* **516**, 511 (2004).
- [11] A. Hillas, *Proc. 19th ICRC, La Jolla*, **3**, 445 (1985).
- [12] D. Heck *et al.*, *Forschungszentrum Karlsruhe Report FZKA 6019* (1998).
- [13] R. S. Fletcher, T. K. Gaisser, P. Lipari, & T. Stanev, *Phys. Rev. D* **50**, 5710 (1994).
- [14] S. Ostapchenko *et al.*, *Proc. 29th ICRC, Pune*, **7**, 135 (2005).
- [15] A. W. Strong, I. V. Moskalenko & O. Reimer, *Astrophys. J.*, **613**, 956 (2004).
- [16] P.S. Coppi & F. A. Aharonian, *Astrophys. J.*, **487**, L9 (1997).
- [17] I. V. Moskalenko, T. A. Porter, S. W. Digel, *Astrophys. J.*, **652**, L65 (2006).
- [18] M. Aguilar *et al.*, *Physics Reports* **366**, 331 (2002).
- [19] S. W. Barwick *et al.*, *Astrophys. J.*, **498**, 779 (1998).
- [20] M. A. DuVernois *et al.*, *Astrophys. J.*, **559**, 296 (2001).
- [21] S. Torii *et al.*, *Astrophys. J.*, **559**, 973 (2001).
- [22] J. Chang *et al.*, *Nature*, **456**, 362-365 (2008).